Tensile Performance of Inter-Module Connections for Modular Steel Buildings Using Finite Element Method

Umi Arifatuus Shoifah[a], Nur Ahmad Husin[a], Yuyun Tajunnisa[a*]

[a] *Department of Civil Infrastructure Engineering, Sepuluh Nopember Institute of Technology, Surabaya, 60116, Indonesia*
[*] *Corresponding author: yuyun_t@its.ac.id*

Abstract

Steel modular construction is an innovative technology that uses prefabricated volumetric module units manufactured in a factory and assembled on site via inter-module connections. However, this system's application in high-rise buildings is limited because the structural performance is strongly influenced by the inter-module connection mechanism. This technology uses a translational spring model to transfer loads between modules through inter-module connections. This approach uses threaded steel rod components, connection plates, shear keys, shear plates, and tie plates. This research aims to determine the maximum tensile capacity of the connection. It also aims to study stress distribution due to tensile forces and failure modes in vertical modular connections. This research uses the finite element method (FEM) to perform numerical analysis by applying monotonic loads. Simulation results indicate that the connection's maximum tensile capacity is 307.48 kN, distributed among two rods with capacities of 153.74 kN each at a displacement of 23.2 mm. The rod undergoes elastic deformation up to Fy = 900 MPa, followed by a plastic phase up to nearly Fu = 1,100 MPa, causing permanent strain and necking. Tensile failure occurred due to plasticity and necking conditions.

Keywords: Inter-module connection; FEM; Tensile Capacity; Failure mode

1. Introduction

Modular steel construction is an innovative building technology that uses prefabricated volumetric modules, which are entirely manufactured in a factory and assembled on-site using inter-module connections to construct fully functional buildings, a general view is provided in

Figure 2 [1], [2]. The use of modular construction can reduce construction time by up to 50% and save costs by up to 20%. Based on previous project case studies [3], the application of modular construction in high-rise buildings remains limited [4], [5], due to several challenges, such as the lack of design guidelines, strong inter-module connection techniques, and insufficient understanding of the structural behaviour and stability of modular buildings [6]. Inter-module connections play a crucial role in withstanding lateral loads acting on modular building structures [7]. Bolted and welded connections are the most commonly used types due to their high strength and efficiency in the manufacturing process [8], [9]. However, their use on-site requires more time and can affect the building's aesthetics due to the large number of bolts [10]. Therefore, the development of innovative module-to-module connections is a key challenge in supporting the future development of modular steel buildings.

A translational spring model has been developed and can be generalised for all inter-module connections by calculating the stiffness properties of structural components at the connection. As this type of connection has been developed in research [6], [11], [12], [13], this connection type can be classified as semi-rigid, as shown in

Figure 2**.** The development of a tie rod connection system for prefabricated (offsite) modular steel buildings aims to transfer lateral forces to damping systems such as core walls or bracing frames, precisely align columns between upper and lower modules, and enhance connection stiffness and stability. Additionally, all three use components such as threaded rods, base plates, and shear keys designed for easy on-site installation, and demonstrate potential in improving structural performance, including energy dissipation capacity and prevention of local buckling Figure 1.

Based on the direction of the connection, connections between modules can be divided into vertical and horizontal connections [14].

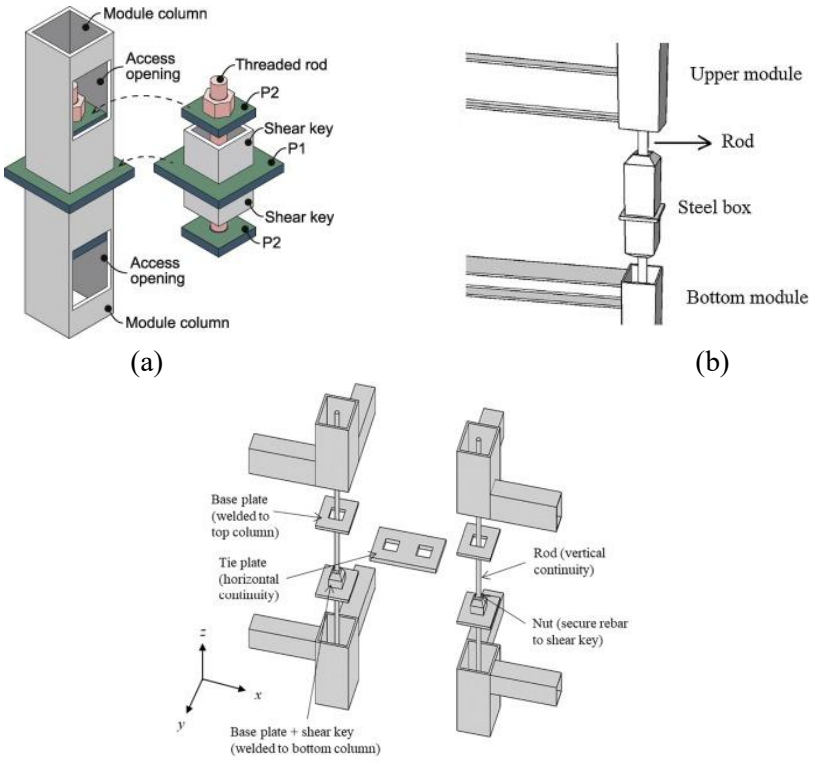

Figure 1. Steel structure inter-module connection model: (a) Proposed post-tensioned vertical inter-module connection detail [11] ; (b) Vertical post- tensioned connection [12]; (c) Post-tensioned rod [15]

The development of a simplified yet realistic connection model is crucial for accurately analysing the global seismic behaviour of high-rise modular steel buildings, as researched by [16]. These connections are expected to be able to withstand the stress and strain caused by axial tensile and shear forces on modular connections. Some considerations in selecting these connections include: a simple connection system to expedite installation, enhancing workplace safety, suitability for tall buildings with appropriate seismic resistance systems, and cost-efficiency as they do not require numerous bolts or welding. Based on the development of research on steel modular connections, this study continues the research [16] to analyse the behaviour of high-rise modular structural connections using Finite Element Method (FEM) numerical simulation. Structural performance, particularly in modular systems, is greatly influenced by non-linear responses and semi-rigid joint behaviour. Therefore, numerical analysis using the Finite Element Method is required to evaluate stress distribution, deformation, ductility, and structural and joint capacity more accurately than linear analysis approaches [17], [18], [19]. This study aims to determine the maximum tensile capacity, stress due to tensile force, and failure mode in modular structural connections.

Figure 2. Modular steel building construction process [20] *:* (a) Factory prefabricated units; (b) Units transportation; (c) Units field assembly; (d) Overall extension completed

(a) (b) (c) (d)

Figure 3. Engineering applications of modular buildings [21]: (a) Houshenshan hospital, Wuhan; (b) Jinghai ziya white collar apartment, Tianjin; (c) Drivelines stuidos residental building, South Africa; (d) Brooklyn B2 residental building New York

2. Inter-Module Connection Configuration

This connection consists of tie plate, shear plate, and shear key elements, which lock the horizontal movement of columns between modules, while vertical connections use rod bars. The force generated by one upper column is transferred by the top plate element and received by the shear key, which is connected to the lower column through the bottom plate. The rod used to connect the columns requires a Lower Plate and Upper Plate as supports for the rod. The configuration of the modular steel connection is shown in Figure 4.

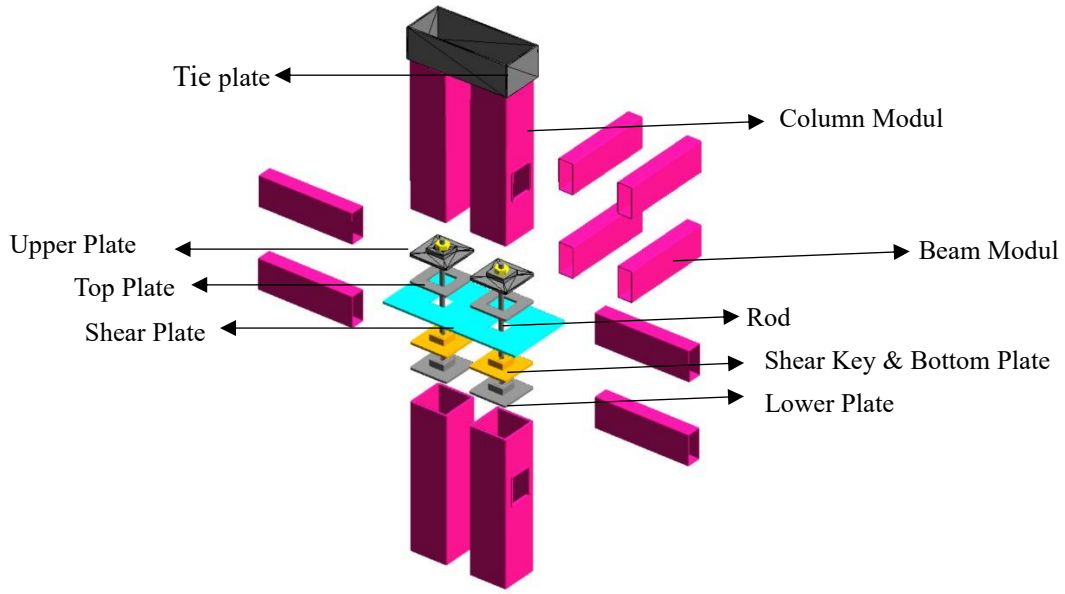

Figure 4. Proposed inter-module connection of steel structure [16]

In general, tie rod connections undergo elastic deformation until they reach the material's yield point. After that, plastic deformation occurs, leading to tensile failure. Common failure modes in tie rod connections include yield failure in the tie rod bar, shear failure in the bolt, and tear-out failure in the tie plate or other connecting components. When the joint is under tensile force, the rod will resist the tensile force, and the length of the rod will increase in proportion to the tensile force in the inter-floor structure.

3. Methodology

The force transfer mechanism of the joint under load and the influence of various parameters on its structural behaviour were investigated using ANSYS 19.2 finite element software. In this finite element model (FEM), three types of non-linearity, namely material non-linearity, geometric non-linearity, and contact non-linearity, were modelled. In monotonic testing, tensile force was applied to the joint specimen until failure occurred [20]. The tensile testing scheme for the joint is shown in Figure 5.

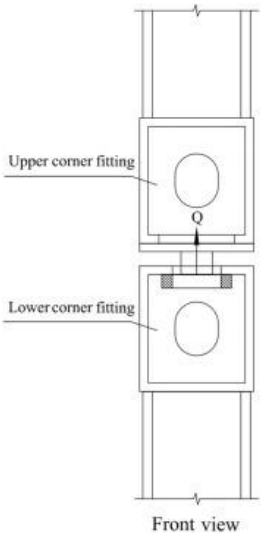

Figure 5. Tensile performance scheme [20]

3.1. Materials

This connection applies the concepts of tie plates and shear keys, where tie plates lock the horizontal movement of columns between modules at the same level. Shear keys and shear plates lock the horizontal movement of columns between modules at different levels, while vertical connections use rod bars. The force generated by one upper column is transmitted by the top plate element and received by the shear key connected to the lower column through the bottom plate. The rod bars used are only sufficient to connect the columns, so a Lower Plate and Upper Plate are required as supports for the rod bars [16]. The connection materials used in previous research [16] are shown in Table 1.

Table 1. Material properties of inter-module connections [16].

Type	Grade	Dia. mm	Thickness mm	Fy MPa	Fu MPa	Ultimate elongation δ (%)	E N/mm²	Weld angle mm	Weld groove FE60XX (mm)
Modular column SHS 250 X 250	S235	-	16	235	400	24	200000	-	-
Upper Plate	S235	-	10	235	400	24	200000	5	-
Bottom Plate	S235	-	20	235	400	24	200000	-	14
Top Plate	S235	-	20	235	400	24	200000	-	14
Lower Plate	S235	-	10	235	400	24	200000	5	-
Shear key SHS 100 X 100	S235	-	5	235	400	24	200000	-	5
Shear Plate	S235	-	10	235	400	24	200000	-	-
Tie Plate	S235	-	8	235	400	24	200000	-	-
Rod	F10T	15	-	900	1100	14	200000	-	-
Tie Nut	-	70	-	621	827	2	170000	-	-

3.2. Stress-strain for steel materials

The stress-strain model for steel materials under elastic conditions forms a linear line, and the Young's modulus (elastic modulus) can be calculated using Hooke's law [22], where according to AISC 360-16, the Young's modulus of steel can be taken as 200,000 MPa. The stress-strain model for steel materials in general, for computational calculations such as the Finite Element Method (FEM), uses a simplified stress-strain model, namely the elasto-plastic model. In this study, to determine the stress-strain curve and strain hardening area, a mathematical model approach using the Ramberg-Osgood model was used. Ramberg-Osgood [23]. The Ramberg-Osgood mathematical model begins by calculating the uniform strain (Ɛus) Equation 2.1 and the Ramberg-Osgood exponent (n) Equation 2.2.

$$\varepsilon_{us} = \left(\frac{\varepsilon_r}{100} - \frac{F_u}{E}\right) x\ 100 \quad (1)$$

$$n = \frac{LN\left(\frac{\varepsilon_{us}}{\varepsilon_p}\right)}{LN\left(\frac{F_u}{F_y}\right)} \quad (2)$$

With :

ε_r = Strain rupture

Fu = Ultimate Tensile Strength (MPa)

Fy = Yield Strength (MPa)

ε_p = Offset yield strain = 0.2%

Then calculate the engineering stress (σeng) – strain (εeng) curve.

$$\varepsilon_{eng} = \frac{\sigma}{E} + 0{,}002\ x\left(\frac{\sigma}{F_y}\right)^n \quad (3)$$

Finally, calculate the true stress (σtrue) – strain (Ɛtrue) curve.

$$\sigma_{true} = \sigma_{eng}\ x(1 + \varepsilon_{eng}) \quad (4)$$

$$\varepsilon_{true} = LN\ x(1 + \varepsilon_{eng}) \quad (5)$$

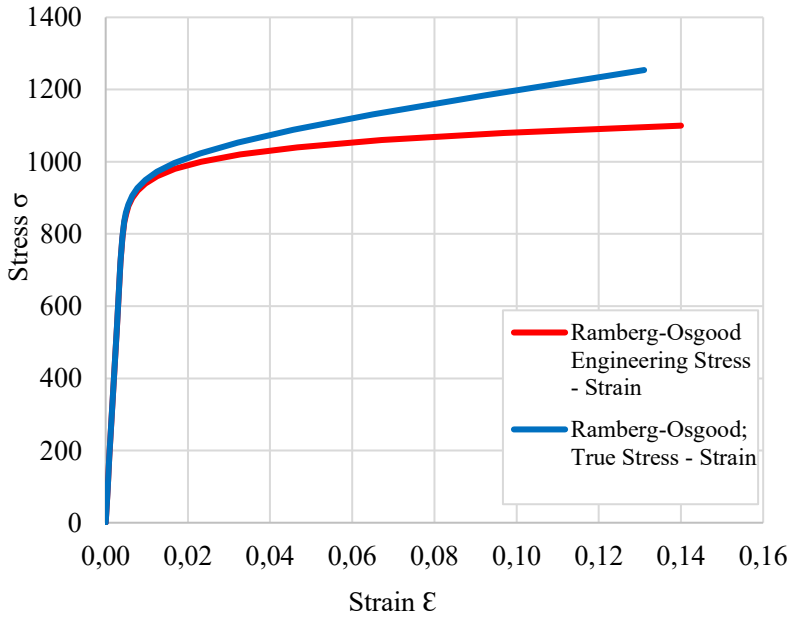

Figure 6. Rod stress-strain curve

Figure 6 and Figure 7 show the Ramberg-Osgood stress-strain curve model for modular columns. Engineering stress-strain Equation 2.3 is the relation between stress and strain calculated based on the initial cross-sectional area and initial length of the test specimen. Meanwhile, true stress-strain Equation 2.4 – Equation 2.5 is the relation between stress and strain calculated based on the current cross-sectional area and actual length change during deformation. In ANSYS simulations involving material plasticity, it is recommended to use true stress-strain. This enables accurate modelling of non-linear behaviour after yielding.

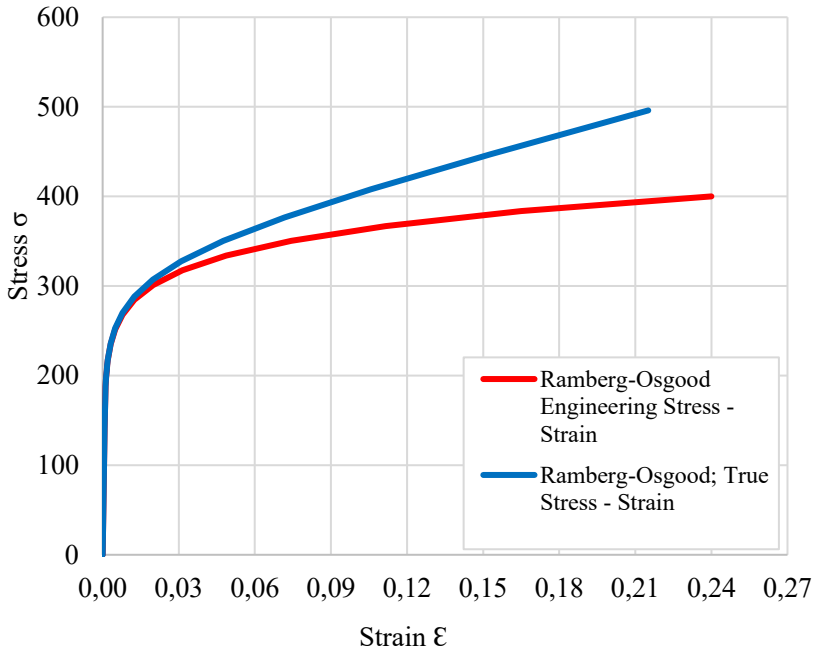

Figure 7. Stress-strain curve of S235

3.3. Numerical model of inter-module connection

The connection load was applied using the displacement control method, in which the load was applied in the form of gradual displacement to the specimen. The tensile force that occurred was recorded as a response to the displacement, so that the load-displacement relationship and the failure behaviour of the connection could be analysed comprehensively. The appropriate mesh density for each component was selected to ensure accuracy and minimise calculation time. The mesh element size is 57 mm for columns and 5 mm for the joint area Figure 8.

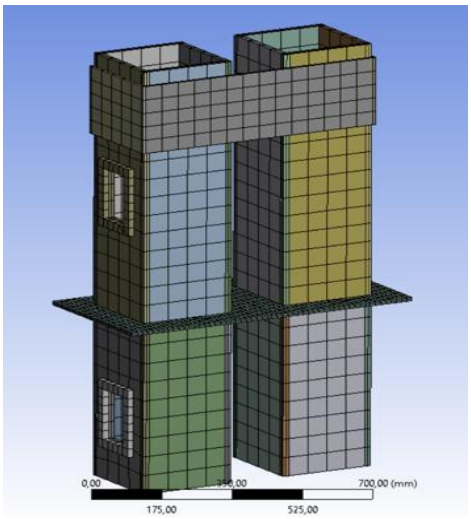

Figure 8. Meshing in joint modelling

The contact types in this model consist of bonded, frictionless, and friction. Bonded contact is used when the elements in this contact simulate two surfaces that are permanently bonded together, without allowing any relative movement (either separation or slip) between them. Loads can be transferred in both the normal and tangential directions. Frictionless contact allows surfaces to slide past each other without resistance (zero friction), but prevents penetration (overlapping) of one another. Loads can only be transferred in the normal direction (compression). Frictional contact, on the other hand, allows surfaces to press against and slide past each other, with friction resistance defined by the coefficient of friction. Surfaces will stick together and resist slipping until the applied tangential force exceeds the friction limit (calculated by multiplying the coefficient of friction by the normal force). Once the friction limit is exceeded, slipping occurs.

Welded connection components, nuts with rods, are modelled using contact bonding. Frictionless contact types connect the modular columns to the shear plates, while frictional contact types connect the connection plates to the rod holes, with a frictional coefficient value of 0.2. To define the tensile test, the load placed on the column surface is controlled using displacement control in the Y direction (perpendicular to the column). The X and Z coordinate systems, as well as the X, Y, and Z rotations, are locked at '0', as shown in Figure 9.

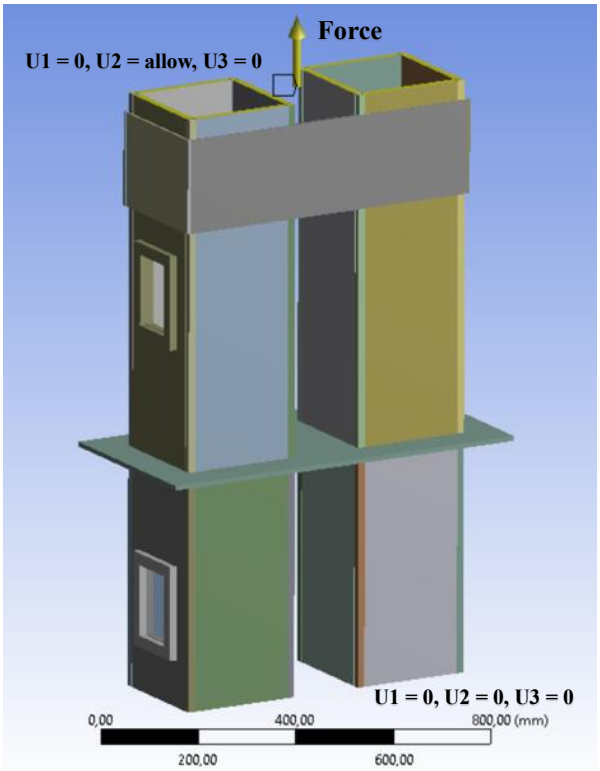

Figure 9. Proposed connection, boundary conditions and points of the displacement

4. Results and Discussion

4.1. Stress distribution

Figure 10 shows the distribution of Equivalent Stress (von Mises) from the FEM simulation, with maximum stress occurring on the upper plate, bottom plate, rod, and nut. However, on the column profile, shear plate, and shear key, the stress is relatively low, indicated by the blue colour, with stress values below the material's yield strength (Fy = 235 MPa), the yield strength of the structural steel column material. This indicates that the axial tensile load is predominantly distributed through the rod and effectively transmitted to the connection.

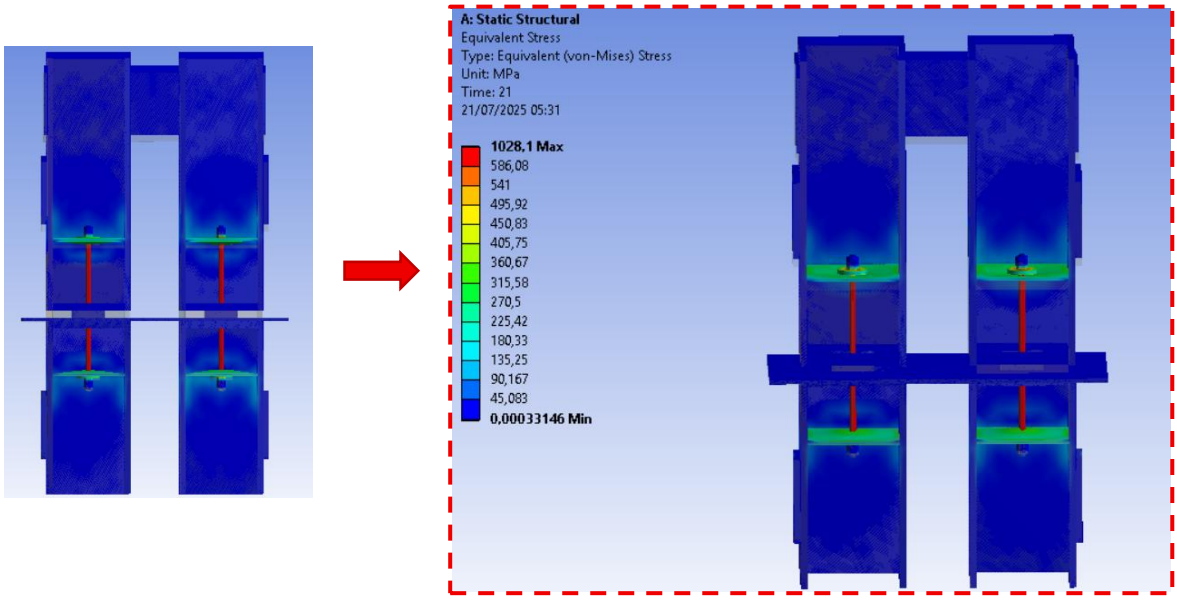

Figure 10. Stress contour of 21.4 mm displacement joint

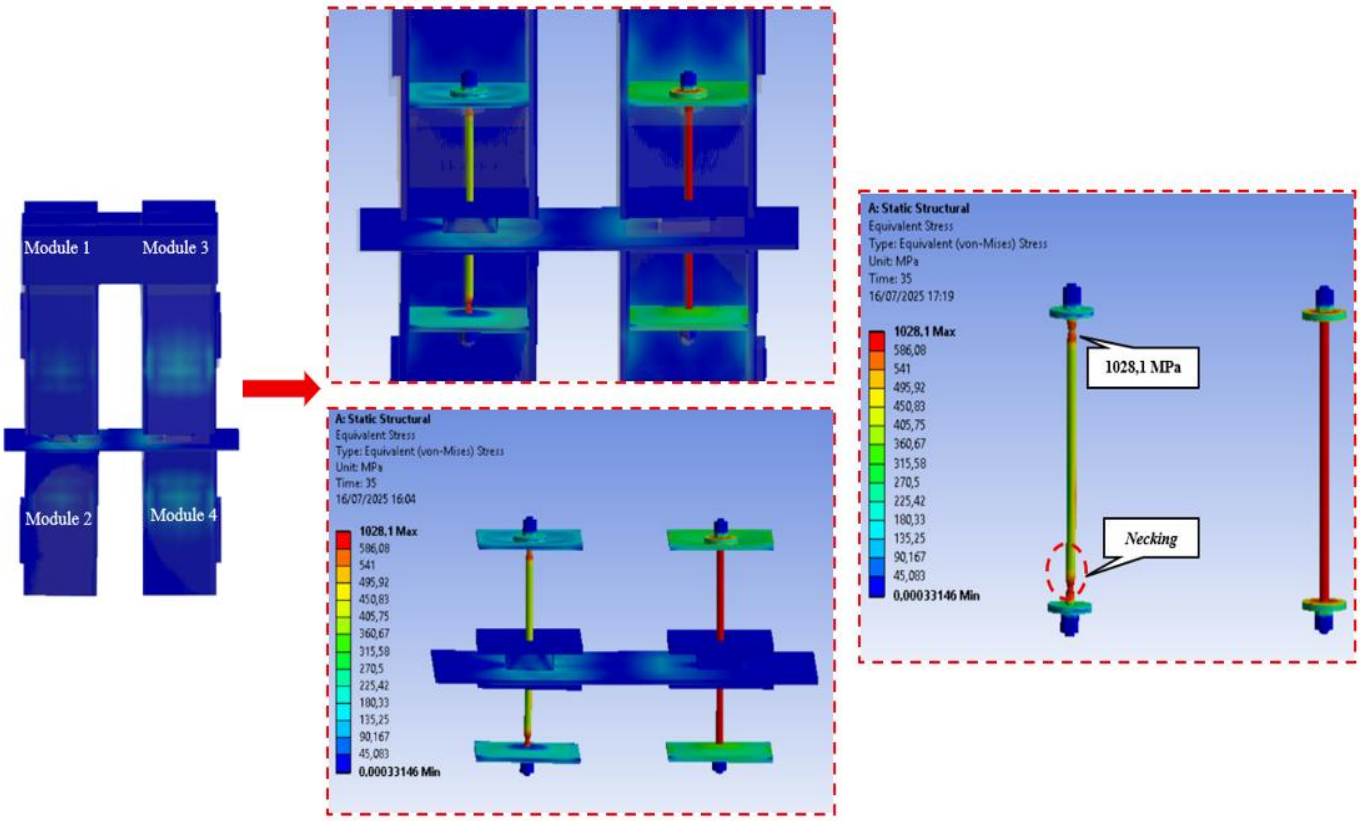

Figure 11. Stress distribution at the connection under tension conditions

Displacement was increased to 35 mm until the stress approached the Fu rod of 1100 MPa Figure 11. The stress at a displacement of 35 mm is 1028.1 mm. From the FEM simulation results, one of the rods connecting Module 1 and Module 2 experienced necking. This occurs when the cross-sectional area of the steel begins to narrow locally due to excessive plastic deformation, reaching the yield stress and approaching the ultimate stress. Based on the simulation

results, it can be concluded that the stress conditions on the rod, upper plate, and lower plate have failed. Therefore, the results of this FEM analysis can be considered valid as a validation of the force distribution corresponding to the material capacity of each component.

4.2. Load-Displacement Curve

Figure *12* shows the load-displacement curve, which illustrates the relationship between the tensile force received by the rod and the deformation that occurs during loading. From displacement 0 mm to 4.7 mm, the load increases linearly from 0 kN to 172.17 kN, indicating that the rod material is still operating within the elastic zone in accordance with Hooke's law, and the stress formed remains below the yield stress (Fy 900 MPa). From displacement 4 to 23 mm, the load increases from 172.17 kN to 307.48 kN, followed by the curve gradient beginning to curve and decrease, indicating that the rod material has begun to exceed the elastic limit and enter the plastic zone, where stress approaches Fy and plastic strain begins to form, resulting in some permanent deformation. At a displacement of 23–35 mm, the joint has fully entered the plastic condition, where stress approaches Fu 1100 MPa and the maximum force of 307.48 kN is reached at a displacement of 23.2 mm. As displacement increases to 35 mm, the load does not increase because the material has entered the strain hardening stage and is experiencing local narrowing (necking).

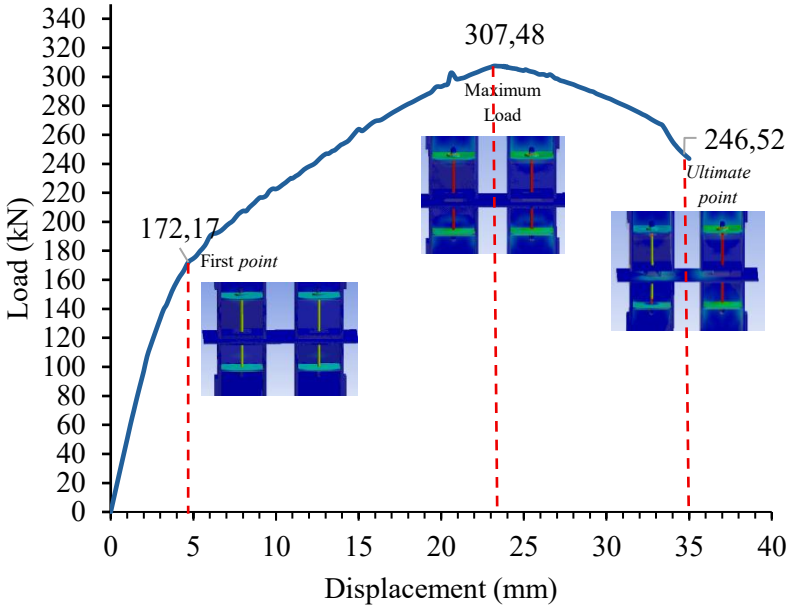

Figure 12. Load-displacement curve of tensile test

The load-displacement curve results from the FEM simulation show the behaviour of the joint when subjected to gradual loading. The curve illustrates the material behaviour of the joint, starting from the elastic zone, through the plastic zone, and approaching the fracture strain. The total tensile load from the simulation results falls between the design allowable capacity and the maximum tensile capacity. Therefore, the material behaviour from the FEM results is acceptable; however, to meet the design safety limits, the joint must be designed such that the working tensile load does not exceed the design allowable capacity.

5. Conclusions

Based on the simulation results using the Finite Element Method (FEM) on the semi-rigid modular connection model, the following results were obtained:

1. The maximum tensile capacity of the connection is 307.48 kN, which is divided between two module columns, so that the tensile capacity per rod reaches 153.74 kN at a displacement of 23.2 mm.
2. The stress-strain behaviour shows that the rod operates elastically up to Fy = 900 MPa, then plastically up to near Fu = 1100 MPa, resulting in permanent strain and necking at maximum displacement (35 mm).

3. The load-displacement curve relationship in the tensile test on the FEM model aligns with the tensile behaviour of steel material, from the elastic zone, through the plastic zone, to the fracture strain condition.
4. The failure mode of the connection occurs due to the material reaching full plasticity in the rod, as the stress approaches the material's Fu value, leading to necking caused by tensile force.

Acknowledgment

The author would like to thank the lecturers for their assistance in conducting this case study and would also like to thank the Building Materials and Structures Laboratory (LMSG), Department of Civil Infrastructure Engineering, Sepuluh Nopember Institute of Technology.

References

[1] Y. Yu and Z. Chen, "Rigidity of corrugated plate sidewalls and its effect on the modular structural design," *Eng. Struct.*, vol. 175, no. August, pp. 191–200, 2018.

[2] F. W. Shi, Y. Ding, L. Zong, W. Pan, Y. Duan, and T. Y. Ping, "Seismic behavior of high-rise modular buildings with simplified models of inter-module connections," *J. Constr. Steel Res.*, vol. 221, no. July, p. 108867, 2024.

[3] N. Bertram, S. Fuchs, J. Mischke, R. Palter, G. Strube, and J. Woetzel, "Modular construction: From projects to products," *Cap. Proj. Infrastruct.*, no. June, pp. 1–30, 2019, [Online]. Available: https://www.mckinsey.com/industries/capital-projects-and-infrastructure/our-insights/modular-construction-from-projects-to-products

[4] S. Shan and W. Pan, "Structural design of high-rise buildings using steel-framed modules: A case study in Hong Kong," *Struct. Des. Tall Spec. Build.*, vol. 29, no. 15, pp. 1–20, 2020.

[5] Z. Wang, W. Pan, and Z. Zhang, "High-rise modular buildings with innovative precast concrete shear walls as a lateral force resisting system," *Structures*, vol. 26, no. November 2019.

[6] J. Y. R. Liew, Y. S. Chua, and Z. Dai, "Steel concrete composite systems for modular construction of high-rise buildings," *Structures*, vol. 21, no. February, pp. 135–149, 2019.

[7] T. Gunawardena, "Behaviour of Prefabricated Modular Buildings Subjected to Lateral Loads Performance evaluation of engineered timber View project," no. December, pp. 0–1, 2016, [Online]. Available: https://www.researchgate.net/publication/322040294

[8] S. Srisangeerthanan, M. J. Hashemi, P. Rajeev, E. Gad, and S. Fernando, "Review of performance requirements for inter-module connections in multi-story modular buildings," *J. Build. Eng.*, vol. 28, no. November 2019.

[9] C. Dan-Adrian and K. D. Tsavdaridis, "A comprehensive review and classification of inter-module connections for hot-rolled steel modular building systems," *J. Build. Eng.*, vol. 50, no. November 2021, p. 104006, 2022.

[10] C. Yang, B. Xu, J. Xia, H. Chang, X. Chen, and R. Ma, "Mechanical Behaviors of Inter-Module Connections and Assembled Joints in Modular Steel Buildings: A Comprehensive Review," *Buildings*, vol. 13, no. 7, 2023.

[11] A. W. Lacey, W. Chen, H. Hao, K. Bi, and F. J. Tallowin, "Shear behaviour of post-tensioned inter-module connection for modular steel buildings," *J. Constr. Steel Res.*, vol. 162, no. November, 2019.

[12] R. Sanches, O. Mercan, and B. Roberts, "Experimental investigations of vertical post-tensioned connection for modular steel structures," *Eng. Struct.*, vol. 175, no. July, pp. 776–789, 2018.

[13] R. A. Sanches, "Development of Vertical Post-tensioned Connection for Modular Steel Buildings by Development of Vertical Post-tensioned Connection for Modular," no. September, 2022.

[14] F. W. Shi, Y. Ding, L. Zong, Y. Chen, and Y. Wu, "Shear behaviour of vertical inter-module connection with bolts and shear keys for MSCs," *Structures*, vol. 47, no. April 2022.

[15] Y. S. Chua, J. Y. R. Liew, and S. D. Pang, "Modelling of connections and lateral behavior of high-rise modular steel buildings," *J. Constr. Steel Res.*, vol. 166, p. 105901, 2020.

[16] Kurniawan et al., “Perencanaan Struktur Gedung Modular Baja 23 Lantai Menggunakan Sistem Ganda Rangka Pemikul Menengah Dikombinasikan Dengan Baja Struktur Bresing,” 2024.

[17] M. S. Darmawan *et al.*, “Comparative Study Of Flexural Performance Of Geopolymer And Portland Cement Concrete Beam,” vol. 23, no. 95, pp. 1–9, 2022.

[18] Y. N. Wibowo, B. Piscesa, and Y. Tajunnisa, “Numerical Investigation Of Geopolymer Reinforced Concrete Beams Under Flexural Loading Using Finite,” vol. 37, no. 1, pp. 27–32, 2022.

[19] Y. Tajunnisa, M. Chadaffi, V. Ramadhaniawan, and R. Pemikul, “Perbandingan Evaluasi Kinerja Bangunan Gedung Tahan Gempa antara Metode SRPMM dan SRPMK SRPMK (Sistem Rangka Pemikul ditentukan dari peninjauan gaya daerah yang ditentukan pada SNI,” vol. 12, pp. 1–16, 2014.

[20] Z. Chen, J. Wang, J. Liu, and Z. Cong, “Tensile and shear performance of rotary inter-module connection for modular steel buildings,” *J. Constr. Steel Res.*, vol. 175, p. 106367, 2020.

[21] A. Zhang, J. Liu, Z. Chen, and T. Chen, “Bending behavior of detachable tapered-head bolt inter-module connection of steel modular structure,” *J. Constr. Steel Res.*, vol. 220, no. May, p. 108829, 2024.

[22] L. Gardner, X. Yun, A. Fieber, and L. Macorini, “Steel Design by Advanced Analysis: Material Modeling and Strain Limits,” *Engineering*, vol. 5, no. 2, pp. 243–249, 2019.

[23] A. T. Diputra, B. Suswanto, Y. Tajunnisa, and H. S. Masiran, “Analisis Numerik Sambungan Baja Reduced Beam Section pada Sumbu Lemah Kolom Menggunakan Program Bantu ANSYS,” vol. 22, pp. 295–306, 2024.